International Journal of Astrobiology 13 (4): 366–377 (2014)
doi:10.1017/S1473550414000378

Gypsum-hosted endolithic communities of the Lake St. Martin impact structure, Manitoba, Canada: spectroscopic detectability and implications for Mars

T. Rhind[1], J. Ronholm[2], B. Berg[1], P. Mann[1], D. Applin[1], J. Stromberg[3], R. Sharma[1], L.G. Whyte[2] and E.A. Cloutis[1]

[1]*Department of Geography, University of Winnipeg, Winnipeg, Manitoba R3B 2E9, Canada*
e-mail: e.cloutis@uwinnipeg.ca
[2]*Department of Natural Resource Sciences, McGill University, Sainte-Anne-de-Bellevue, Quebec H9X 3V9, Canada*
[3]*Department of Earth Sciences, Centre for Planetary Science and Exploration, University of Western Ontario, London, Ontario N6A 5B7, Canada*

Abstract: There is increasing evidence that Mars may have once been a habitable environment. Gypsum is targeted in the search for Martian biosignatures because it can host extensive cryptoendolithic communities in extreme terrestrial environments and is widespread on Mars. In this study the viability of using different spectroscopy-based techniques to identify the presence of gypsum endolithic communities was investigated by analysing various cryptoendoliths collected from the Lake St. Martin impact crater (LSM), a Mars analogue site found in Manitoba, Canada. Concurrently, the cryptoendolithic microbial community structure present was also analysed to aid in assigning spectroscopic features to microbial community members. Two main morphologies of endolithic communities were collected from gypsum deposits at LSM: true cryptoendolithic communities and annular deposits on partially buried boulders and cobbles <1 cm below the soil surface. Endolithic communities were found to be visibly present only in gypsum with a high degree of translucency and could occur as deep as 3 cm below the exterior surface. The bacterial community was dominated by a phylum (*Chloroflexi*) that has not been previously observed in gypsum endoliths. The exterior surfaces of gypsum boulders and cobbles are devoid of spectroscopic features attributable to organic molecules and detectable by reflectance, Raman, or ultraviolet-induced fluorescence spectroscopies. However, exposed interior surfaces show unique endolithic signatures detectable by each spectroscopic technique. This indicates that cryptoendolithic communities can be detected via spectroscopy-based techniques, provided they are either partially or fully exposed and enough photon–target interactions occur to enable detection.

Received 28 April 2014, accepted 7 August 2014

Key words: biosignature, cryptoendolith, gypsum, Mars, Raman, spectroscopy

Introduction

Mars is a geologically diverse body that contains hydrous minerals, including a variety of phyllosilicates and hydrous sulphates (e.g. Murchie *et al.* 2009; Carter *et al.* 2013). Hydrous minerals are high-priority targets for exploration because their presence is consistent with historical warmer, wetter and possibly habitable environmental conditions (Farmer & Des Marais 1999; Summons *et al.* 2011). One of the most plentiful hydrous-sulphate minerals found on Mars is gypsum. Gypsum is a major component of an extensive dune field and sublimation tills in Olympia Planitia (Langevin *et al.* 2005; Massé *et al.* 2010). It has also been detected in Juventae Chasma and Iani Chaos (Gendrin *et al.* 2005; Sefton-Nash *et al.* 2012), in Mawrth Vallis (Wray *et al.* 2010), the Columbus crater (Wray *et al.* 2011), and as veins along the rim of Endeavour Crater in the Cape York area (Squyres *et al.* 2012). More recently gypsum has been identified as a probable vein fill in Gale crater (Grotzinger *et al.* 2013). Exposure of gypsum to Mars surface conditions indicates that gypsum is stable on the surface of present-day Mars (Cloutis *et al.* 2007, 2008).

On present-day Mars, organic compounds exposed to the unfiltered solar radiation and oxidizing surface conditions are rapidly destroyed or altered (e.g. Stoker & Bullock 1997). However, when life arose on the Earth ~3.8 Gyr ago, environmental conditions were probably similar to the environmental conditions experienced on early Mars, 3.5–4.0 Gyr ago (Davis & McKay 1996; McKay 1997; Holm & Andersson 2005; Cockell *et al.* 2010; Edwards 2010). Subsequent changes in the terrestrial and Martian environment would have caused organisms to adopt various survival strategies, such as the colonization of new habitats and the adaptation of suitable protective mechanisms and strategies (Martinez-Frias *et al.* 2006; Villar *et al.* 2006;

Edwards 2010). If life had previously existed on Mars before the planet became a cold desert, these organisms may have been similar to those living in extreme environments on present day Earth, and taken refuge in gypsum as cryptoendoliths (McKay 1997; Raulin & McKay 2002; Simoneit 2004; Delaye & Lazcano 2005; Edwards 2010). Chemical traces of these extinct microbial cells may have survived the Martian surface shielded within rocks (Stoker & Bullock 1997; Dartnell *et al.* 2012; Dartnell and Patel 2013; de Vera *et al.* 2013; Poch *et al.* 2013; Stromberg *et al.* 2014). Thus, there is interest in developing techniques that are able to detect biosignatures left by extinct cryptoendolithic communities for Martian exploration.

While the search for evidence of present or extinct life beyond our planet drives planetary exploration, terrestrial analogue sites are heavily used in the development of techniques and tools that facilitate extraterrestrial exploration (Hughes & Lawley 2003; Canfield *et al.* 2004; Dong *et al.* 2007; Douglas *et al.* 2008; Panieri *et al.* 2008, 2010; Cockell *et al.* 2010; Stivaletta *et al.* 2010; Gomez *et al.* 2012; Schopf *et al.* 2012; Allwood *et al.* 2013; Battler *et al.* 2013). Analogue sites are used to determine the limits of terrestrial life (Preston & Dartnell 2014). Terrestrial cryptoendolithic communities present in Mars analogue sites are examined for insights into what may have been the last habitable environment on Mars (McKay 1997; Cady *et al.* 2003).

Endolithic niches in evaporite deposits are of astrobiological interest given their potential for preserving biomarkers (Cockell *et al.* 2002, 2005; Barbieri & Stivaletta 2011; Schopf *et al.* 2012; Poch *et al.* 2013). There is also the possibility that they can provide long-term habitable microenvironments, even in very environmentally harsh conditions (Panieri *et al.* 2010). In addition, conditions within rocks can provide microenvironments that provide a number of essential requirements for life (Hughes & Lawley 2003; Canfield *et al.* 2004; Gomez *et al.* 2012; Kelly *et al.* 2012).

Gypsum can host extensive cryptoendolithic communities due to its light colour, softness, translucency and porosity (Dong *et al.* 2007; Wierzchos *et al.* 2011; Ziolkowski *et al.* 2013). The translucency of gypsum allows for photosynthesis and nitrogen fixation; although, it still provides protection from ultraviolet (UV) radiation. Gypsum's porosity provides protection from extreme temperatures and desiccation (Friedmann 1982; Boison *et al.* 2004). Gypsum can provide microbes with sufficient water to survive by retaining moisture, and this is especially relevant in polar deserts and hyper-arid climates (Wierzchos *et al.* 2006). These factors may account for the high biodiversity found in gypsum-hosted communities, relative to other cryptoendolithic communities (Garbary *et al.* 1996; Seckback 1999). Colonization of the gypsum subsurface provides protection against environmental conditions (Villar *et al.* 2006), and although terrestrial analogue environments are less harsh, analogues share characteristics in common with current day Mars (Martinez-Frias *et al.* 2006).

Endolithic microorganisms can form biofilms. These biofilms are particularly resilient to extreme environmental stress and can be made up of heterogeneous communities including bacteria, fungi and eukaryotic microalgae (Sigler *et al.* 2003). In addition to biofilm formation, endolithic microorganisms may synthesize various biomolecules that serve as protection against environmental stress. These can include photoprotective and light-harvesting pigments, such as chlorophylls, bacteriochlorophylls and carotenoids (Wynn-Williams *et al.* 1999; Cogdell *et al.* 2000; Squier *et al.* 2004; Villar *et al.* 2006). Biomolecules exhibit unique spectral features, and as such, can be detected and differentiated by various spectroscopic techniques (Wynn-Williams *et al.* 1999; Villar *et al.* 2006).

An analogue study of gypsum deposits in the Lake St. Martin (LSM) impact crater was conducted. Terrestrial crater-hosted gypsum deposits are poorly understood and gypsum is shown to be a pervasive mineral that can be found on Mars. The search for evidence of extraterrestrial life currently relies on spectroscopic detection of mineralogical assemblages indicative of habitable conditions or biosignatures at the planetary surface (Bell *et al.* 2003; Milliken *et al.* 2010; Squyres *et al.* 2012). The aim of this work was to examine geo-biological relationships focusing on factors controlling the presence of endoliths, cryptoendolithic community structure and endolith detectability by different spectroscopic techniques. Many of the instruments used in this study (UV-induced fluorescence spectroscopy, Raman spectroscopy and reflectance spectroscopy) are analogous to instruments present on planned and future Mars missions involving rovers (e.g. Pancam on the Mars Exploration Rovers, Mastcam on the Mars Science Laboratory and a Raman spectrometer on the 2018 ExoMars rover). A number of investigative techniques have been applied to detecting evidence of past or present life in terrestrial analogue environments.

Methods

Study site

LSM is a circular ~23 km diameter impact structure located in central Manitoba, Canada (Fig. 1). It is similar to the Endeavour crater on Mars (which is currently being explored by the Opportunity Mars Exploration Rover) in size (Squyres *et al.* 2012) and both contain gypsum in or near the crater (Cloutis *et al.* 2011); therefore, LSM is considered an excellent Mars analogue site, especially for the study of intracrater evaporites (Cloutis *et al.* 2011). LSM formed ~228 Ma (Schmieder *et al.* 2013) when a hypervelocity asteroid collided with ~400–500 m of Ordovician and Devonian sandstones, shales and carbonates superimposed on Archaean-aged granite (McCabe & Bannatyne 1970; Bannatyne & McCabe 1984). The impact resulted in the near-total volatilization of carbonates and impact melting of granite (McCabe & Bannatyne 1970), creating a complex crater (Bannatyne & McCabe 1984). Present crater depth (from surface to intact bedrock) is ~320 m; however, prior to glacial modification, the crater depth may have been up to 610 m (McCabe & Bannatyne 1970). The intracrater evaporite member of interest overlies and grades into a red bed member and is a 43 m thick sequence of gypsum/anhydrite, minor glauberite and occasional interbedded clays (Bannatyne 1959; McCabe & Bannatyne 1970). The age of gypsum/anhydrite deposits are unknown,

https://doi.org/10.1017/S1473550414000378 Published online by Cambridge University Press

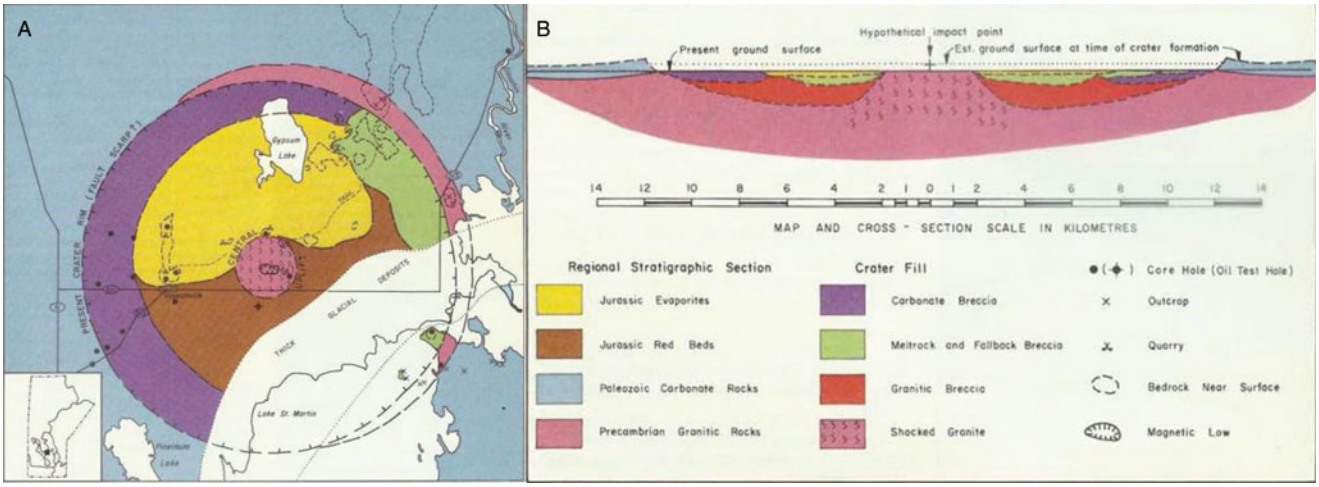

Fig. 1. Regional map of the St. Martin impact structure, Manitoba, Canada.

although the regional evaporite upper Amaranth formation (which has been identified as Jurassic), is often inferred to have concurrent deposition (McCabe & Bannatyne 1970); however the evidence for this association is controversial (Leybourne *et al.* 2007). A series of open pit gypsum mines in the area have exposed a continuous ~5 km long section of the gypsum/anhydrite deposit of up to 15 m vertical exposure. The exposed gypsum exhibits highly variable grain size and depositional morphology, a variety of weathering textures (Bannatyne 1959), glacial morphological modification (expressed as drag folds) (Wardlaw *et al.* 1969), variable scale folding (likely due to hydration/dehydration of gypsum/anhydrite) and karst features such as sinkholes.

Sample collection

Samples were collected from gypsum deposits within LSM in June 2012 and transported to the University of Winnipeg for analysis. Rock hammers were used to expose the gypsum endoliths in boulders. After examining different areas within the impact crater, endoliths were found to be concentrated in intact rocks, as opposed to partially weathered and friable rocks or outcrops, suggesting the need for a stable substrate for endolith survival. Endoliths were aseptically collected and stored frozen until analysis. Samples were hand crushed and dry sieved for spectroscopic analysis.

Sample descriptions

A survey of gypsum–endolith associations in the field showed wide variations in the visual appearance of endolithic communities. Gypsum competence was associated with the presence of visible endolithic communities. Cryptoendoliths generally consisted of at least two layers: an upper red-orange layer and a middle green layer (Fig. 2). Occasionally a blue layer was observed as well, usually just below the green layer. Depths and thicknesses of these layers varied widely, and some of the coarser-grained gypsum samples were found to have coloured bands as deep as 3 cm beneath the uppermost surface. Extensive endolithic communities were also found at the interface between rocks and the surrounding eroded gypsum soil, usually at a depth of <1 cm.

DNA extraction and 16S rRNA sequencing

DNA extraction and 16S rRNA sequencing was conducted on the samples in order to be able to better relate any spectroscopic features to specific endolithic community members. The detailed results and description of this aspect of our study is the subject of a forthcoming paper. Briefly, DNA was extracted from 0.5 g of each sample by hand crushing each rock type with a sterile mortar and pestle. After crushing the rocks, a hot phenol method was used for DNA extraction, briefly: CTAB buffer (500 µl) and lysozyme (50 mg ml^{-1}) were added to each of the samples and incubated at 60°C for 30 min. Then 10 µl of proteinase K (20 mg ml^{-1}) and RNAse A (10 mg ml^{-1}) were added and the samples were returned to incubate at 60°C for 30 min. After incubation 20 µl of β-mercaptoethanol was added to each sample and incubation was continued for 10 min. A phenol:-chloroform:isoamyl alcohol (25:24:1) (300 µl) mixture which had been pre-heated to 60°C was added to each sample and gently mixed. Each sample was centrifuged at 13000 rpm for 30-min. The aqueous layer was transferred to a fresh 1.5 ml tube and an additional 300 µl of hot phenol:chloroform:isoamyl alcohol was added to the aqueous layer and mixed. The suspension was centrifuged at 13800 rpm for 30 min. The upper aqueous layer was transferred to a clean tube and two volumes of 100% molecular grade ethanol cooled to −20°C, were added. The samples were gently mixed and incubated overnight at −20°C. Each sample was then centrifuged at 13000 rpm for 30 min at 4°C. The supernatant was discarded and the pellet was washed in 70% ethanol until phenol was undetectable. The pellet was dried for 30 min and then re-suspended in DEPC water.

DNA was sequenced using the Roche 454 FLX and TITANIUM Genome Sequencer at Research and Testing Laboratories LLC (Lubbock, Texas, USA). Pyrosequencing targeted the 16S rRNA gene of Bacteria and Archaea using the 28F/592R and 314F/958R primer sets, respectively. In addition, the presence of Fungi was examined using the Fungal Selective Assay, which relies on the primer pair ITS1F/ITS4R.

https://doi.org/10.1017/S1473550414000378 Published online by Cambridge University Press

Fig. 2. Images of the gypsum-hosted cryptoendoliths used in this study.

Bioinformatic analysis

The MOTHUR software suite was used for the analysis of 454 GSFLX data (Schloss *et al*. 2009). The standard operating procedures suggested by Schloss *et al.* (2011) were followed for analysis of bacterial, archaeal and fungal sequences with minor modifications.

Reflectance spectroscopy

Reflectance spectra of gypsum endoliths were measured at the University of Winnipeg HOSERLab on spots (~5–10 mm in diameter) on the naturally exposed outer rock surfaces as well as several interior surfaces where the endoliths were exposed by sample collection. These interior endolithic surface regions were selected and distinguished based on community colour (orange, green, blue) as well as endolith-free (white). Reflectance spectra were acquired with an ASD Field Spec Pro HR spectrometer (0.35–2.5 µm) with a 50 W QTH light source with a viewing geometry of i=30° and e=0°. Spectra were measured relative to a calibrated Spectralon® standard; 1000 spectra were collected and averaged to improve signal-to-noise ratio (SNR).

Ultraviolet-induced fluorescence spectroscopy

The UV-induced fluorescence emission spectra of gypsum samples were measured at the University of Winnipeg HOSERLab using an Ocean Optics S-2000 lab spectrometer. It is configured to acquire high-resolution (~0.3 nm resolution) spectra in the 200–860 nm range. Bidirectional spectra at i=30° and e=0° were acquired. A Spectralon standard was used to set exposure times and to minimize the presence of any spectral artefacts. Integration times for the fluorescence measurements were 10 s. Illuminated spot sizes were of the order of a few millimetres, which enabled measurements of individual colour bands in the samples. Samples were analysed directly with no additional preparation and were chosen based on the colours and abundance of the endoliths. As with the reflectance measurements, fluorescence spectra were acquired for white (endolith-free) surfaces and different coloured endolith layers. Fluorescence was induced using a 70 mW 405 nm laser (Wicked Lasers, Tsim Sha Tsui, Kowloon, Hong Kong) with a 10 mm glass diffuser to allow for a sufficiently large area of the sample to be illuminated.

Raman spectroscopy

Raman spectra were collected at the University of Winnipeg HOSERLab over the 175–4000 cm^{-1} range at a resolution of ~4 cm^{-1} at 614 nm with the B&WTek (Newark, DE) i-Raman-532-S instrument. Excitation was provided by a 532 nm ~50 mW BWN solid-state diode laser. Scattered light was detected by a Glacier™ *T*, a high spectral resolution (~0.08 nm) thermal electrically cooled (14°C) charged-couple device (CCD) detector. The automatic integration time function (which increases integration time incrementally, until the response is close to saturation) was used, yielding an optimal SNR. Sample measurements were acquired with the BAC102 fibre optic with a working distance of 5.9 mm, which gives a theoretical spot size of 85 µm. The BAC102 fibre optic probe contains a long-pass OD6 notch filter, which filters reflected excitation light prior to interaction with the detector for an increased SNR. Samples were placed on an adjustable stage and were approached directly to the distance regulator prior to collection. Measurements for each sample were made by first acquiring

https://doi.org/10.1017/S1473550414000378 Published online by Cambridge University Press

a dark current spectrum, followed by measurement of the sample. Both measurements were made using an identical viewing geometry and integration time, and 20 averaged spectra. Raman-shift calibration was monitored through regular measurements of a polystyrene standard.

A DeltaNu Rockhound Raman spectrometer was used for complementary data collection in the 200–2000 cm^{-1} range. The instrument uses a thermoelectrically cooled (0°C) CCD detector and a solid-state diode laser of 100 mW at 785 nm. Theoretical spot size measured by the instrument is 25 µm. The instrument has a long pass OD6 notch filter. A spectral resolution of 7 cm^{-1}, an optimized integration time approaching signal detector saturation and 20 averaged spectra were used to increase the SNR within each sample. The Rockhound instrument was mounted securely with the probe pointed 90° downwards. Samples were placed on an adjustable stage and were approached directly to the probe prior to collection. Prior to each sample collection, the instrument was calibration checked with a polystyrene standard.

Results

Microbial community identification

As mentioned, detailed discussion of the composition of the endolithic community structure is the subject of a forthcoming paper. However, a broad overview of the community structure is important for assisting in assigning any spectroscopic features to specific community members. The endolithic community was examined by pyrosequencing with various primers and analysing the sequences using the Mothur software suite. Sequences were assigned to operational taxonomic units (OTUs), using a max difference of two base pairs and classified to the Phylum level (Fig. 3(a)). In general, *Chloroflexi* and *Proteobacteria* were the dominant phyla in each of the samples. The Shannon index indicated that bacterial α-diversity was similar in each endolith sample (GYQ-001 3.23, GYQ-007 3.15, GYQ-008 2.98 and GYQ-011 3.14). Several bacterial OTUs where shared between samples (Fig. 3(b)), GYQ-001 and GYQ-008 had richness of 63 and 46 OTUs, respectively; 31 of these OTUs overlapped between these two communities making them the most similar cryptoendolith samples in this study. Each of the samples produced several internal transcribed spacer (ITS) sequences. However, all ITS sequences were classified as either *Ascomycota, Basidiomycota* or were unclassified (Fig. 3(c)). The Shannon scores were similar for each of the Gypsum samples (GYQ-001 2.22, GYQ-007 1.57, GYQ-008 2.31 and GYQ-011 2.44) and indicated that fungal diversity was lower than bacterial diversity within these gypsum-hosted communities. Archaeal DNA was not present in GYQ-001, GYQ-007 or GYQ-011 samples. After processing, there were 9622 archaeal sequences in GYQ-008 that grouped to a single OTU and were identified to the family level as *Nitrososphaeraceae* (Fig. 3(d)).

UV/VIS/NIR reflectance spectroscopy (350–2500 nm)

The reflectance spectra of the samples are dominated by absorption features characteristic of gypsum, regardless of the region of the sample from which the data were taken, or the presence of endolithic communities (Fig. 4). Spectra of both the external gypsum surface and the coloured interior endolithic communities are nearly identical above 800 nm. The exterior surface spectra are free of any identifiable organic absorption bands, indicating that the exterior surface is not conducive to microbial colonization (Garbary *et al.* 1996). The primary absorption features observed are consistent with gypsum's expected complex H_2O overtone/combination feature at ~1390–1534 nm, and doublet at ~1944/1970 nm, as well as other less prominent features associated with the SO_4 tetrahedra and other H_2O overtones and combinations (Cloutis *et al.* 2006).

As mentioned, the only significant features in the spectra that can be confidently attributed to biology are seen below 800 nm. In this range, the spectra of the endolithic communities exposed in the interior of the samples show a sharp decrease in absolute reflectance, with major absorption features at ~440 and ~670 nm, a minor feature at ~640 nm and shoulders at ~500 and 580–600 nm. These features vary in intensity (depth) and width depending on the colour of the endolithic community, as is observed in Fig. 4. Spectral variations between samples outside of this wavelength region can largely be attributed to factors such as surface roughness, grain size variations and perhaps degree of hydration. Multiple spectra of different endolith layers were acquired, and each colour group has broadly similar spectra; spectral variations between different samples can again be attributed to differences in surface roughness and grain size, as well as density of microbes.

The primary features at 450 and ~670 nm are attributable to absorption by chlorophyll-*a*, and the shoulder at ~500 nm is indicative of carotenoids, a family of orange-coloured UV-protectant pigments (Richardson 1995; Quesada *et al.* 1999; Merzlyak *et al.* 2003). The orange layer, likely due to a concentration of carotenoids, shows no readily-observable spectral features attributable to chlorophyll.

This interpretation of the spectral features below 800 nm correlates with what is observed in hand samples (Fig. 2), the colour of the pigments, and absorption spectra of the dominant phyla in the endolithic communities. For green endolithic samples, the abundance of the green photosynthetic chlorophyll-*a* pigment produces the strong absorption features at ~670 and 450 nm. While these chlorophyll features are evident in all samples, they are most prominent in the green-coloured layer spectra. The endolith layers that appear blue have the most prominent feature at ~640 nm, which corresponds to the bluish pigment phycocyanin (Richardson 1995). This also applies to the orange endolithic communities, which have a broad and more evident ~500 nm feature due to absorption by orange UV-protectant carotenoid pigments.

The reflectance spectra show some features consistent with the presence of *Chloroflexi*, specifically minor absorption features in the 460–510 nm region (most evident in the blue layer spectrum) (Vasmel *et al.* 1986; Botero *et al.* 2004), 770 nm (most evident in the orange layer spectrum) and 870 nm (most evident in the green layer spectrum) (Vasmel *et al.*

https://doi.org/10.1017/S1473550414000378 Published online by Cambridge University Press

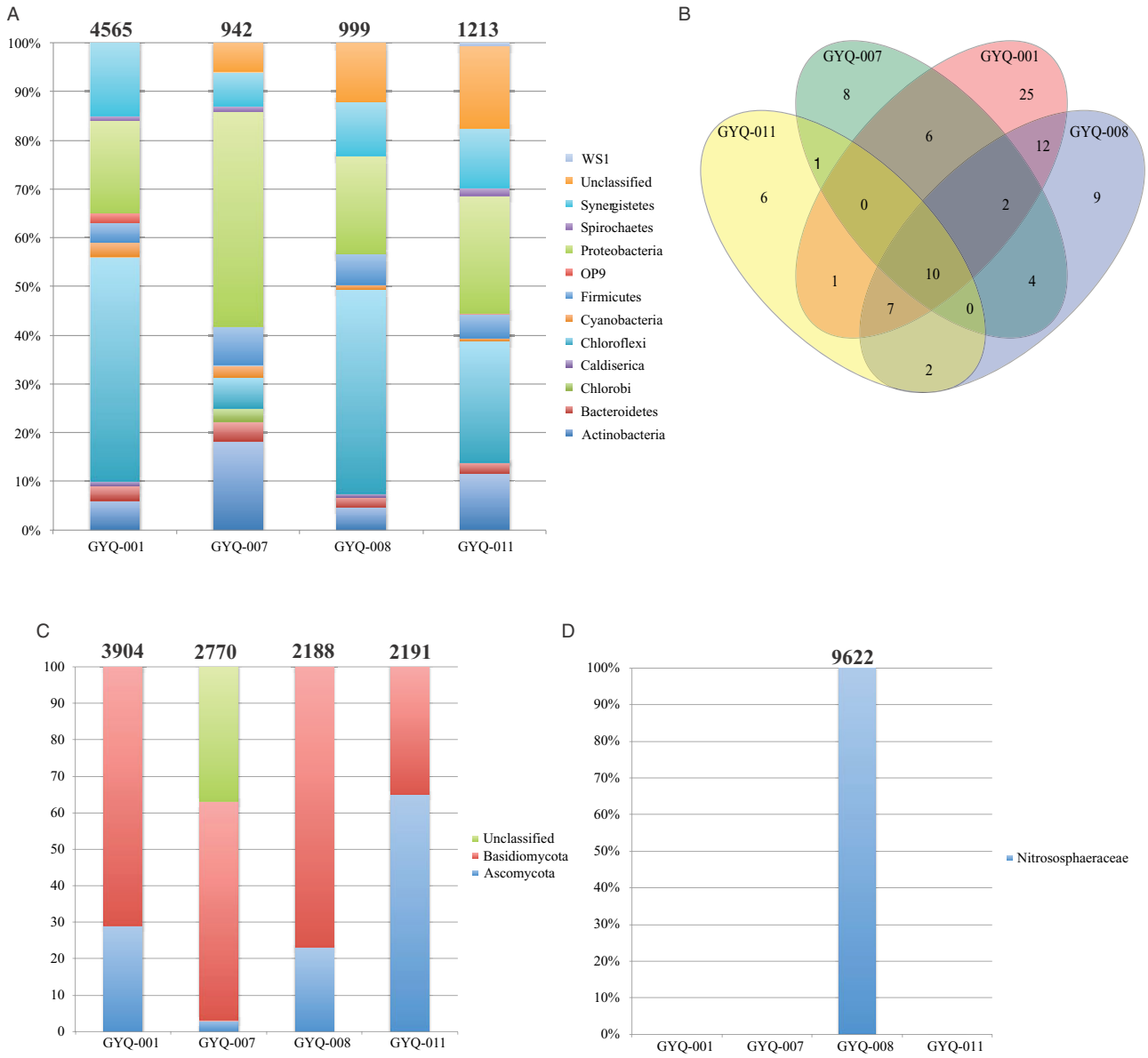

Fig. 3. Gypsum-hosted cryptoendolith community profile based on pyrosequencing the 16S rRNA or ITS regions. (a) Bacterial diversity is displayed at phylum level. (b) In addition to having several phyla shared between samples, several OTUs are common to one or more samples. (c) The fungal community is also shown at phylum level and is dominated by *Basidiomycota* and *Ascomycota*. (d) Archaeal sequences were only identified in GYQ-008 and only 1 OTU was present; therefore, archaeal sequences are displayed to the genus level. The numbers shown above each community profile are indicative of how many sequences were used to generate the profile.

1986; Boomer *et al.* 2002) and stronger absorption bands near 430, 580 and 670 nm (Botero *et al.* 2004; Bryant *et al.* 2007). Given the diversity of *Chloroflexi* species, we do not expect to see all potential absorption features (e.g. absorption features at 460–520 and 740 nm are not evident in our spectra (Vasmel *et al.* 1986; van Amerongen *et al.* 1988).

Absorption features consistent with the presence of *Proteobacteria* include absorption features near 410 nm (most evident in the blue and green layer spectra), 560 nm (possibly present in the blue and green layer spectra superimposed on a stronger 580 nm band) other potential absorption features, in the 800–830 nm region (Gall *et al.* 1999) are not evident. We note that in solid samples, such as these, absorption features are generally broader than those in liquid absorption spectra and can also be shifted in wavelengths relative to the same molecules *in vivo*. That, combined with the multiplicity of possible chromophores, greatly complicates assignment of specific absorption features to specific phyla or biomolecules. Therefore, confident assignment of spectral features to unique mechanisms is generally not warranted.

UV-induced fluorescence spectra

The UV-induced fluorescence spectra show some similarities and differences. The exterior surfaces of endolith-containing boulders showed no fluorescence peaks beyond 440 nm; the broad peak between ~410 and 600 nm is attributable to gypsum (Fig. 5). The green endoliths layers showed fluorescence peaks near 480 and 670–680 nm. Blue endolith layers showed

https://doi.org/10.1017/S1473550414000378 Published online by Cambridge University Press

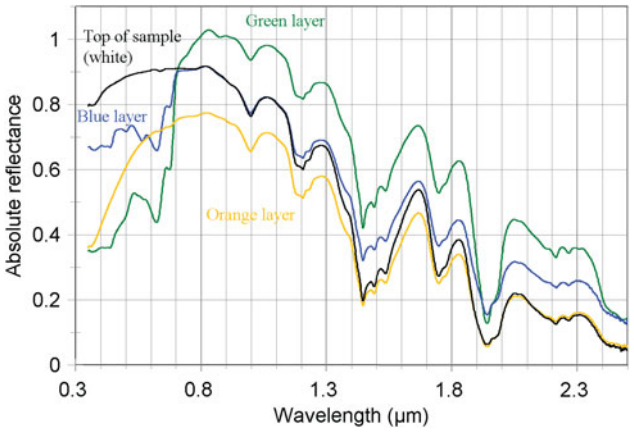

Fig. 4. Reflectance spectra (350–2500 nm) of different endolith layers in the gypsum sample and exterior sample surface.

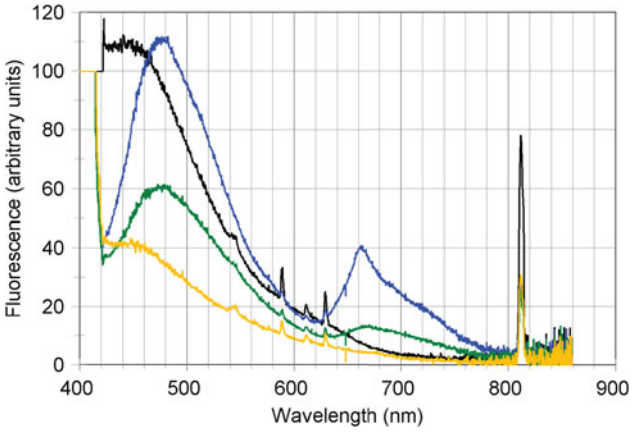

Fig. 5. UV-induced fluorescence spectra of different endolith layers in the gypsum samples, and exterior sample surface.

fluorescence peaks near 480 and 660–670 nm, whereas orange layers only showed a weak fluorescence peak near 450, similar to the exterior gypsum surfaces, and a possible weak peak near 680 nm. The fluorescence peak near 680 nm is characteristic of green photosynthetic chlorophyll-*a* (Richardson 1995) as well as carotenoids (Kleinegris *et al.* 2010) and in our spectra it extends beyond 700 nm, as expected for chlorophyll-*a* (Kraus & Weis 1991 and references therein). Sharp peaks between 590 and 650 nm are spectral artefacts, whereas the sharp peak at 810 nm is an overtone of the laser wavelength.

Potential fluorescence peaks associated with *Chloroflexi* and *Proteobacteria* are expected near 525, 610, 670, 760 nm and in the 800–860 nm interval (van Amerongen *et al.* 1991; Shibata *et al.* 2007; Choi *et al.* 2010). Of these, the 610 nm peak appears to be present with a narrow profile as is seen in the emission spectra of *Proteobacteria* in aqueous solutions (Choi *et al.* 2010). A peak in the 660–670 nm region is also seen in the endolith spectra, while other peaks, expected near 525, 760 and 800–860 nm are not evident (e.g. Vasmel *et al.* 1986). These results, again suggest that endoliths can be recognized by the presence of, usually, more than one emission feature, but precise microbial, and even some specific molecular, assignments may not be feasible.

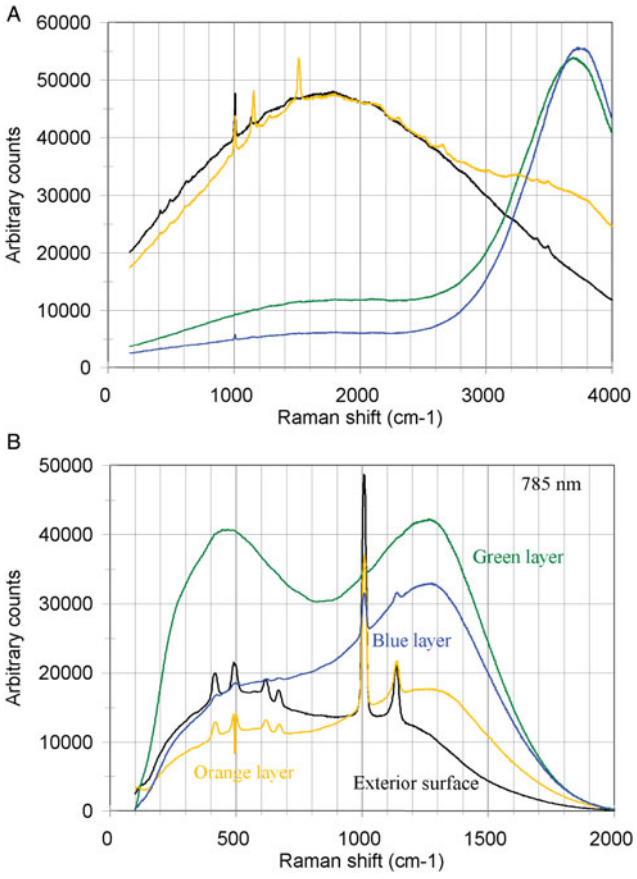

Fig. 6. Raman spectra of different endolith layers in the gypsum samples and exterior sample surface. (a) 532 nm Raman spectra and (b) 785 nm Raman spectra.

Raman spectra

Gypsum exhibits a large number of Raman active peaks, with the strongest bands being present near 415, 495, 671, 1006, 1132 and 3400–3500 cm^{-1} (Krishnamurthy & Soots 1971; Edwards *et al.* 2005a). Cyanobacteria and *Proteobacteria* have prominent Raman peaks at a large number of frequencies (Gall *et al.* 1999; Edwards *et al.* 2005a), and cyanobacterial endoliths in gypsum can be identified using differences in Raman peak positions.

Our 532 nm Raman spectra of the gypsum and the endolith layers are dominated by fluorescence (Fig. 6(a)). The most prevalent Raman peak is located near 1006 cm^{-1} and is associated with gypsum. It should be noted that the endolith layers in our samples do not always exhibit 100% areal coverage by cyanobacteria, and consequently, gypsum will contribute to the Raman signal. The unpopulated gypsum shows the expected gypsum Raman peaks (Krishnamurthy & Soots 1971; Berenblut *et al.* 1973). The orange layer exhibits a gypsum-associated peak near 1006 cm^{-1}, as well as additional peaks near 1160 and 1520 cm^{-1}, which are associated with beta-carotene (Edwards *et al.* 2005b). The Raman spectra of the green and blue (cyanobacterial) layers are dominated by fluorescence attributable to chlorophyll, and the only Raman peak is the strongest gypsum peak near 1006 cm^{-1}. The position of the fluorescence peaks of these two endolith layers differ somewhat ($\sim$3680 versus $\sim$3720 cm^{-1}).

https://doi.org/10.1017/S1473550414000378 Published online by Cambridge University Press

The 785 nm Raman spectra show different behaviour than the 532 nm Raman spectra (Fig. 6(b)). The exterior surface and orange layer Raman spectra show more well-resolved gypsum-associated peaks: near 415, 495, 620, 670, 1006 and 1132 cm^{-1}. All the endolith layer spectra exhibit the 1006 cm^{-1} gypsum peak, and some show additional weaker gypsum peaks. The orange layer spectrum does not show the expected beta-carotene peaks near 1160 and 1520 cm^{-1}. The fluorescence spectra are also more diverse, with broad peaks near 450 and 1250 cm^{-1} in the endolith layer spectra. Evidence for the endoliths in the Raman spectra is very variable. The main organic molecules expected to be present in our samples are chlorophyll-*a* and carotenoids. The strongest Raman peaks associated with chlorophyll-*a* are near 1100–1700 cm^{-1}, and are attributable to C–C and C–N stretching modes (Lutz 1974; Robert *et al.* 1999; Campanella *et al.* 2000; Kubo *et al.* 2000). There is no strong evidence in our spectra for a chlorophyll-*a* Raman feature.

Discussion

Microbial community

The phyla *Actinobacteria, Bacteriodetes, Chloroflexi, Cyanobacteria, Firmicutes* and *Synergistetes* were found in each sample. Some of these phyla can include photosynthesizing bacteria that have photochemical chlorophyll-based or bacteriochlorophyll-based reaction centres (Lim 2002; Bryant & Frigaard 2006). Carotenoids, found in phototrophs and some non-photosynthetic bacteria, function as accessory pigments used for light-harvesting in photosynthesis and protection from photo-oxidative damage (Lim 2002; Edwards *et al.* 2003). Bacterial pigments are likely responsible for some of the colour variation observed between gypsum samples.

Based on the detection of the 16S rRNA gene, gypsum-hosted cryptoendolithic communities from LSM showed more bacterial richness than previously documented in similar studies. Gypsum crusts in Tunisia had populations that included *Cyanobacteria, Actinobacteria, Proteobacteria, Bacteroidetes, Deinococus* and *Flavobacteria*; however, population evenness varied between samples as a result of *Cyanobacteria* dominance (<15 to >80%) (Stivaletta *et al.* 2010). In hyper-arid environments (Atacama Desert, the Mojave Desert and Al-Jafr Basin) gypsum community evenness was also variable since *Cyanobacteria* dominated (79%) the Al-Jafr Basin population and represented only 18% of the Mojave Desert population (Dong *et al.* 2007). Gypsum cryptoendoliths from the Canadian high Arctic had a population consisting of *Cyanobacteria, Actinobacteria, Proteobacteria* and *Acidobacteria* that was dominated by *Cyanobacteria* and *Proteobacteria* (Ziolkowski *et al.* 2013). *Cyanobacteria* made up of a comparatively smaller (1–3%) part of cryptoendolith population in the LSM impact structure. The elevated bacterial richness observed in LSM gypsum is partially because of a decrease in *Cyanobacteria* numbers, and could be a result of this being a less hostile environment. However, increased richness could also partially be an artefact of improving sequencing and bioinformatic technologies. Archaea were not detected in the Tunisian crust samples (Stivaletta *et al.* 2010); however, the population of *Nitrososphaeraceae* found in GYQ-008 was consistent with the *Thaumarchaea*-dominated population found in the high Arctic (Ziolkowski *et al.* 2013).

A striking difference between the bacterial cryptoendolithic community in this study and other gypsum-hosted communities is the dominance of the *Chloroflexi* phyla at LSM. *Chloroflexi* was proposed as a phylum in 2001 to succeed 'green non-sulphur' bacteria (Garrity & Holt 2001). Within the sequences grouped in the *Chloroflexi* phyla, OTUs can be further classified as part of the *Anaerolineae, Caldilineae* and *Chloroflexi* classes, although most OTUs group to *Anaerolineae*. Most *Anaerolineae* have been identified through 16S rRNA sequencing from environmental samples, very few have been cultured and cultured isolates are exclusively anaerobic and tend to be thermophilic (Yamada *et al.* 2006). However, novel *Chloroflexi* sequences, associated with temperatures near 0°C were discovered in alpine tundra soil (Costello & Schmidt 2006). These bacteria were likely anoxic and may be using geochemical inputs such as sulphide (Costello & Schmidt 2006). Therefore, given the range of diversity within the *Chloroflexi* phylum and the environmental overlap of our site and the site from Costello & Schmidt (2006), it is not surprising that this phylum was found in these cryptoendoliths. The richness of the microbial communities in our samples provides some benefits and potential detriments for spectroscopy-based astrobiological investigations. Increased species diversity could translate into a larger number of absorption bands in reflectance spectra, emission peaks in fluorescence spectra or emission lines in Raman spectra. Increased species diversity could also, however, translate into broader, and hence less diagnostic, absorption or emission peaks.

Gypsum-hosted communities have been found in some of the most arid conditions on the Earth (Dong *et al.* 2007; Wierzchos *et al.* 2011). As Mars became arid, if they existed, Martian microbes may have taken refuge in gypsum microenvironments. Therefore, gypsum is a good target in the search for biomarkers of extinct Martian life. The degradation of pigments and their derivatives must be taken into consideration before they can be used as biomarkers in the search for extant or extinct life on Mars. Fossilization and preservation of organic material is aided by freezing temperatures, anaerobic-hypersaline conditions and desiccation (Ellery *et al.* 2003). The degradation of carotenoids over geological time occurs by modification of the polyene chain by diverse reactions, in which hydrogenation is the most common, to produce isoprenoids (Ellery *et al.* 2003; Marshall & Marshall 2010). The degradation of chlorophylls, bacteriochlorophylls and haem redox centrer of aerobic metabolism produces porphyrins (Ellery *et al.* 2003; Suo *et al.* 2007). Isoprenoids and porphyrins are considered to be important as biomarkers since they have been found to remain in the fossil record for long periods of time and are indicative of biotic origin (Ellery *et al.* 2003).

Reflectance spectroscopy

The reflectance spectra indicate that it is possible to differentiate between pure gypsum and gypsum-containing endolithic

https://doi.org/10.1017/S1473550414000378 Published online by Cambridge University Press

communities. This can be best achieved by concentrating on the region of the spectra below 800 nm where the absolute reflectance of the endolith-containing gypsum drops significantly. This corresponds to what is known as the red edge of plant leaf reflectance, a measure of chlorophyll content and a marker of photosynthetic biomass (Filella & Penuelas 1994). Below this 800 nm threshold there are multiple observable spectral features that are due to absorption by photosynthetic and UV-protectant pigments (Richardson 1995; Quesada *et al.* 1999; Merzlyak *et al.* 2003).

It should be noted that this red edge can also be attributed to the presence of iron and other mineral features (Seager *et al.* 2005). However, the overall shape of the endolithic spectra below 800 nm with their multiple characteristic absorption features and 'green peak' near 550 nm, collectively are unlike absorption features associated with Fe-bearing minerals (e.g. Morris *et al.* 1985; Sherman & Waite 1985). As mentioned, such absorption bands can often, but not always, be attributed to specific organic molecules (organosomes), but the presence of multiple features would strengthen the case for being attributable to multiple types of organosomes. It does not appear likely that these features could be attributed to specific species or phyla, however. Above the 'red-edge', gypsum completely dominates the spectra and no reliable differentiation can be made between external surface spectra and the internal endolith spectra (Fig. 4).

The Mars Explorations Rovers (MER) Spirit and Opportunity are equipped with a Panoramic Camera (Pancam), which is a multispectral, stereoscopic, panoramic imaging system consisting of two digital cameras. Each camera includes a small eight-position filter wheel to allow surface mineralogical studies in the 400–1100 nm wavelength region, with a number of filter band passes falling below 800 nm (Bell *et al.* 2003). We examined whether differentiation between pure gypsum and endolith-containing gypsum could be made using these filters. The prominent 670 nm endolith feature would have the greatest likelihood of being detected using the L3 filter, which has a central wavelength of 673 nm and a band pass of 16 nm (Bell *et al.* 2003), perhaps appearing as a downward 'kink' relative to the bands on either side. However, detectability would still be hampered by the fact that the 670 nm feature in endolith spectra is quite narrow. The possibility of detection of the spectral features due to biological pigments in gypsum-hosted endolithic communities using Pancam-type spectra is something that has yet to be investigated thoroughly, but preliminary results suggest that it is detectable in endolithic spectra, even after exposure to Mars surface conditions (Stromberg *et al.* 2014).

Fluorescence spectroscopy

The fluorescence spectra that we collected show a clear distinction between white gypsum crust and the different endolithic communities that we could visually detect (Fig. 5). The emission peaks of the endoliths (located near 660–670 nm for the blue endoliths and near 670–680 for the green endoliths) were not present in the gypsum surface spectra. It was difficult to find a completely isolated orange spot on these gypsum samples, as the green bands were often very close to the orange layers. It is possible that the variability in fluorescence spectra of the orange layer is due to the detection of the green endoliths situated nearby, and that the orange layer does not in fact contain endoliths at all. It was hoped that this would be determined via phylogenetic analysis, but we were unsuccessful in isolating the orange and green layers as they were virtually inseparable without contamination from one another. GYQ-001 and GYQ-007 are considered as somewhat of a mixture between green and orange, whereas the blue layer was able to be independently sampled in GYQ-008 and GYQ-011. The overall community structure of the green and orange regions as compared to the blue regions did not appear to show significant differences that are respective to the colours via phylogenetic analysis and this is somewhat reflected in the fluorescent and reflectance spectra. In addition, the fluorescence spectra –while sensitive to various organic molecules – have less distinct emission features which are broader than absorption bands in the reflectance spectra. This suggests that fluorescence spectroscopy, at least as expressed by our endolithic communities, may be less diagnostic than the reflectance spectra for attributing specific mechanisms/organisms/biomolecules to specific fluorescence features.

These results also suggest that gypsum-hosted endoliths may be impossible to detect with surficial techniques due to the overlying endolith-free or endolith-poor gypsum, which is essentially optically thick. However, if access to the interior of a gypsum boulder, outcrop or vein could be provided, UV-induced fluorescence spectroscopy can serve as a rapid screening tool for determining the presence of endoliths which could then be subjected to more detailed analysis using other techniques.

Raman spectroscopy

As discussed above, Raman spectroscopy can provide a high spatial resolution method for detection and identification of organic signatures in gypsum-hosted endoliths (Edwards *et al.* 2005a). Our Raman spectra differ from those of Edwards *et al.* (2005a), who were able to detect a number of cyanobacteria-associated Raman peaks. Our spectra were dominated by fluorescence and the only consistent Raman peak was near 1006 cm^{-1} due to gypsum. We suspect that the sparseness of the endoliths in the sample, coupled with the larger spot size used in our measurements ($\sim$80 μm), and perhaps coupled with a more complex endolithic community in our samples, accounts for the lack of consistent Raman peaks that can be attributed to the microbiology of the samples.

The choice of Raman laser wavelengths has an important impact on experimental capabilities due to various factors, such as broad-band fluorescence and optical coupling (Strommen & Nakamoto 1997). Therefore, to achieve optimum detection of organic peaks, the choice of laser wavelength is important. A shorter wavelength laser ($\sim$532 nm) is a better choice for producing strong Raman emission bands for inorganic molecules and gypsum (Strommen & Nakamoto 1977). Red or near-infrared lasers (660–830 nm) provide better

https://doi.org/10.1017/S1473550414000378 Published online by Cambridge University Press

induced fluorescence suppression. This may prove useful in the Martian context, where targets will likely consist of unknown mixtures. In our study, the 785 nm laser was more suitable for the excitation of Raman spectra than the 532 nm laser.

When comparing the Raman spectra of powdered versus whole rock samples, the 785 nm laser exhibited better Raman spectra bands for the powdered samples in terms of lower induced fluorescence and more Raman peaks visible above background. The 785 nm spectra also exhibited more organic peaks than the 532 nm spectra, especially bands associated with carotenoids. The 532 nm spectra still exhibited satisfactory Raman spectra for powdered and whole samples in comparison to the 785 nm in terms of exhibiting enough Raman peaks to enable determination of the presence of gypsum and organic compounds.

The results have significant importance for the deployment of Raman instrumentation in the forthcoming ExoMars rover mission and for future astrobiology exploration. It must be noted that endoliths are not detectable in unbroken samples, and some way to access the interior of a gypsum sample (at least to as deep as would enable endolith detection) must be provided.

ExoMars has the potential to detect endoliths, as it is equipped with a 532 nm Raman spectrometer, and a drill that can penetrate up to 2 m and provide samples to the Raman spectrometer for interrogation (Lopez-Reyes *et al.* 2013). As demonstrated above, endoliths can be detected in both powdered and whole rock spectra.

A companion study (Stromberg *et al.* 2014) has also found that endolith-associated spectral features undergo variable amounts of change and reduction when exposed to Mars-like surface conditions. Some features, in particular, an absorption feature near 670 nm, and likely associated with chlorophyll, persist even after exposure to Mars surface conditions for long periods of time (equivalent to decades on Mars), albeit with reduced intensities. This suggests that spectroscopic detection of some biomarkers may be possible on Mars for recently exhumed surfaces.

Conclusions

Spectroscopic techniques, in conjunction with the bioassays, provide insights into how the search for similar endolithic communities on Mars can be optimized for detection and characterization. Organic pigments of the types present in our samples are most readily detectable in reflectance and UV-induced fluorescence spectra below 800 nm. Spectral features below 800 nm for both reflectance and UV-induced fluorescence techniques are not seen in the surface spectra of the naturally occurring subaerial surfaces of gypsum directly above the endolithic communities. The lack of an endolithic or organic spectral signature from the exterior gypsum surfaces is attributable to its generally inhospitable nature. On Mars, we expect that any gypsum-hosted cryptoendoliths would exhibit similar behaviour. If endolithic communities could be made spectrally accessible, the ability of reflectance, Raman and fluorescence spectroscopy to detect multiple pigments and differences in their relative abundances, allows interpretations about the community structure and the conditions under which they exist to be made.

References

Allwood, A.C., Burch, I.W., Rouchy, J.M. & Coleman, M. (2013). Morphological biosignatures in gypsum: diverse formation processes of messinian (~6.0 Ma) gypsum stromatolites. *Astrobiology* **13**(9), 870–886.

Bannatyne, B.B. (1959). Gypsum-anhydrite deposits of Manitoba. *Manitoba Mines Branch* **258**, 46.

Bannatyne, B.B. & McCabe, H.R. (1984). Manitoba crater revealed. *GEOS* **13**, 10–13.

Barbieri, R. & Stivaletta, N. (2011). Continental evaporites and the search for evidence of life on Mars. *Geol. J.* **46**, 513–524.

Battler, M.M., Osinski, G.R. & Banerjee, N.R. (2013). Mineralogy of saline perennial cold spring on Axel Heiberg Island, Nunavut, Canada and implications for spring deposits on Mars. *Icarus* **224**, 364–381.

Bell, J.F. *et al.* (2003). Mars exploration rover athena panoramic camera (Pancam) investigation. *J. Geophys. Res.* **108**, 8063. DOI: 10.1029/2003JE002070, E12.

Berenblut, B.J., Dawson, P. & Wilkinson, G.R. (1973). A comparison of the Raman spectra of anhydrite ($CaSO_4$) and gypsum ($CaSO_4.2H_2O$). *Spectrochim. Acta* **29A**, 29–36.

Boison, G., Mergel, A., Jolkver, H. & Bothe, H. (2004). Bacterial life and dinitrogen fixation at a gypsum rock. *Appl. Environ. Microbiol.* **70**(12), 7070–7077.

Boomer, S.M., Lodge, D.P., Dutton, B.E. & Pierson, B. (2002). Molecular characterization of novel red green nonsulfur bacteria from five distinct hot spring communities in Yellowstone National Park. *Appl. Environ. Microbiol.* **68**(1), 346–355.

Botero, L.M., Brown, K.B., Brumefielf, S., Burr, M., Castenholz, R.W., Young, M. & McDermott, T.R. (2004). *Thermobaculum terrenum* gen. nov., sp, nov.: a non-phototrophic gram-positive thermophile representing an environmental clone group related to the Chloroflexi (green non-sulfur bacteria) and Thermomicrobia. *Arch. Microbiol.* **181**, 269–277.

Bryant, D.A. & Frigaard, N.U. (2006). Prokaryotic photosynthesis and phototrophy illuminated. *Trends Microbial* **14**(11), 488–496.

Bryant, D.A. *et al.* (2007). *Candidatus Chloracidobacterium thermophilum*: an aerobic phototrophic acidobacterium. *Science* **317**, 523–526.

Cady, L.S., Farmer, J.D., Grotzinger, J.P., Schopf, J.W. & Steele, A. (2003). Morphological biosignatures and the search for life on Mars. *Astrobiology* **3**(2), 351–368.

Campanella, L., Cubadda, F., Sammartino, M.P. & Saoncella, A. (2000). An algal biosensor for the monitoring of water toxicity in estuarine environments. *Water Res.* **35**, 69–76.

Canfield, D.E., Sørensen, K.B. & Oren, A. (2004). Biogeochemistry of a gypsum-encrusted microbial ecosystem. *Geobiology* **2**, 133–150.

Carter, J., Poulet, F., Bibring, J.P., Mangold, N. & Murchie, S. (2013). Hyfrous minerals on Mars as seen by the CRISM and OMEGA imagine spectrometers: updated global view. *J. Geophys. Res., Planets* **118**, 1–28.

Choi, D.W. *et al.* (2010). Spectral and thermodynamic properties of methanobactin from γ- proteobacterial methan oxidizing bacteria: a case for copper competition on a molecular level. *J. Inorg. Biochem.* **104**, 1240–1247.

Cloutis, E.A. *et al.* (2006). Detection and discrimination of sulphate minerals using reflectance spectroscopy. *Icarus* **184**, 121–157.

Cloutis, E.A., Craig, M.A., Mustard, J.F., Kruzelecky, R.V., Jamroz, W.R., Scott, A., Bish, D.L., Poulet, F., Bebring, J.P. & King, P.L. (2007). Stability of hydrated minerals on Mars. *Geophys. Res. Lett.* **34**, L20202.

Cloutis, E.A., Craig, M.A., Kruzelecky, R.V., Jamroz, W.R., Scott, A., Hawthorne, F.C. & Mertzman, S.A. (2008). Spectral reflectance properties of minerals exposed to simulated Mars surface conditions. *Icarus* **195**, 140–168.

Cloutis, E.A., Berard, G., Mann, P. & Stromberg, J. (2011). The Gypsumville – Lake St. Martin impact structure: Shocked carbonates, intracrater evaporates and cryptoendoliths. In *Analogue sites for Mars*

https://doi.org/10.1017/S1473550414000378 Published online by Cambridge University Press

Special Meeting, the 42nd Annual Lunar and Planetary Science Conference, The Woodlands, Texas. Abstract #6009.

Cockell, C.S., Lee, P., Osinski, G., Horneck, G. & Broady, P. (2002). Impact-induced microbial endolithic habitats. *Meteor. Planet. Sci.* **37**, 1287–1298.

Cockell, C.S., Scheurger, A.C., Billi, D., Friedmann, E.I. & Panitz, C. (2005). Effects of a simulated Martian UV flux on the cyanobacterium, *Chroococcidiopsis* sp. 029. *Astrobiology* **5**(2), 127–140.

Cockell, C.S., Osinski, G.R., Banerjee, N.R., Howard, K.T., Gilmour, I. & Watson, J.S. (2010). The microbe-mineral environment and gypsum neogenesis in a weathered polar evaporite. *Geobiology* **8**, 293–308.

Cogdell, R.J., Howard, T.D., Bittl, R., Schlodder, E., Geisenheimer, I. & Lubitz, W. (2000). How carotenoids protect bacterial photosynthesis. *Phil. Trans. R. Soc. Lond. B Biol. Sci.* **355**(1402), 1345–1349.

Costello, E.K. & Schmidt, S.K. (2006). Microbial diversity in alpine tundra wet meadow soil: novel Chloroflexi from a cold, water-saturated environment. *Environ. Microbiol.* **8**, 1471–86.

Dartnell, L.R. *et al*. (2012). Experimental determination of photostability and fluorescence-based detection of PAHs on the Martian surface. *Meteor. Planet. Sci.* **47**, 806–819.

Dartnell, L.R. & Patel, M.R. (2013). Degradation of microbial fluorescence biosignatures by solar ultraviolet radiation on Mars. *Int. J. Astrobiol.* **13**, 1–12.

Davis, W.L. & McKay, C.P. (1996). Origins of life: a comparison of theories and application to Mars. *Orig. Life Evol. Biosph.* **26**, 61–73.

Delaye, L. & Lazcano, A. (2005). Prebiological evolution and the physics of the origin of life. *Phys. Life Rev.* **2**, 47–64.

de Vera, J.P., Duali, S., Kereszturi, A., Konca, L., Lorek, A., Mohlmann, D., Marschall, M. & Pocs, T. (2013). Results on the survival of cryptobiotic cyanobacteria samples after exposure to Mars-like environmental conditions. *Int. J. Astrobiol.* **13**, 35–44.

Dong, H., Rech, J.A., Jiang, H., Sun, H. & Buck, B.J. (2007). Endolithic cyanobacteria in soil gypsum: occurrences in Atacama (Chile), Mojave (United States), and Al-Jafr Basin (Jordan) deserts. *J. Geophys. Res.* **112** (G2), G02030.

Douglas, S., Abbey, W., Mieke, R., Conrad, P. & Kanik, I. (2008). Textural and mineralogical biosignatures in an unusual microbialite from Death Valley, California. *Icarus* **193**, 620–636.

Edwards, H.G.M. (2010). Raman spectroscopic approach to analytical astrobiology: the detection of key geological and biomolecular markers in the search for life. *Phil. Trans. R. Soc. A* **368**, 3059–3065.

Edwards, H.G.M., Newton, E.M., Wynn-Williams, D.D., Dickensheets, D., Schoen, C. & Crowder, C. (2003). Laser wavelength selection for Raman spectroscopy of microbial pigments *in situ* in Antarctic desert ecosystem analogues of former habitats on Mars. *Int. J. Astrobiol.* **1**(4), 333–348.

Edwards, H.G.M., Jorge Villar, S.E., Parnell, J., Cockell, C. & Lee, P. (2005a). Raman spectroscopic analysis of cyanobacterial gypsum halotrophs and relevance for sulfate deposits on Mars. *Analyst* **130**, 917–923.

Edwards, H.G.M., Moody, C.D., Jorge Villar, S.E. & Wynn-Williams, D.D. (2005b). Raman spectroscopic detection of key biomarkers of cyanobacteria and lichen symbiosis in extreme Antarctic habitats: evaluation for Mars lander missions. *Icarus* **174**, 560–571.

Ellery, A., Kolb, C., Lammer, H., Parnell, J., Edwards, H., Richter, L., Patel, M., Romstedt, J., Dickensheets, D., Steele, A. & Cockell, C. (2003). Astrobiological instrumentation for Mars – the only way is down. *Int. J. Astrobiol.* **1**(4), 365–380.

Farmer, J.D. & Des Marias, D.J. (1999). Exploring for a record of ancient Martian life. *J. Geophys. Res.* **104**(E11), 26977–26995.

Filella, I. & Penuelas, J. (1994). The red edge and shape as indicators of plant chlorophyll content, biomass and hydric state. *Int. J. Remote Sens.* **15**(7), 1459–1470.

Friedmann, E.I. (1982). Endolithic microorganisms in the Antarctic cold desert. *Science* **215**, 1045–1053.

Gall, A., Yurkov, V., Vermeglio, A. & Robert, B. (1999). Certain species of the *Proteobacteria* possess unusual bacteriochlorophyll *a* environments in their light-harvesting proteins. *Biospectroscopy* **5**, 338–345.

Garbary, D.J., Van Thielen, N. & Miller, A. (1996). Endolithic algae from gypsum in Nova Scotia. *J. Phycol.* **32**(Suppl.), 17.

Garrity, G.M. & Holt, J.G. (2001). Phylum BVI. Chloroflexi phy. nov. In *Bergey's Manual of Systematic Bacteriology*, ed. Boone, D.R., Castenholz, R.W. & Garrity, R.W., pp. 427–446. Springer, New York, NY, USA.

Gendrin, A., Mangold, N., Bibring, J-P., Langevin, Y., Gondet, B., Poulet, F., Bonello, G., Quantin, K., Mustard, J., Arvidson, R. & LeMouelic, S. (2005). Sulfates in Martian layered terrains: the OMEGA/Mars express view. *Science* **307**, 1587–1589.

Gomez, F.M. *et al*. (2012). Habitability: where to look for life? Halophilic habitats: earth analogs to study Mars habitability. *Planet. Space Sci.* **68**, 48–55.

Grotzinger, J.P. *et al*. (2013). A habitable fluvio-lacustrine environment at Yellowknife Bay, Gale Crater, Mars. *Science* **10**(1126), 1–17.

Hughes, K.A. & Lawley, B. (2003). A novel Antarctic microbial endolithic community within gypsum crusts. *Environ. Microbiol.* **5**(7), 555–565.

Holm, N.G. & Andersson, E. (2005). Hydrothermal simulation experiments as a tool for studies of the origin of life on earth and other terrestrial planets: a review. *Astrobiology* **5**, 444–460.

Kelly, C.A., Poole, J.A., Tazaz, A.M., Chanton, J.P. & Bebout, B.M. (2012). Substrate limitation for methanogenesis in hypersaline environments. *Astrobiology* **12**(2), 89–97.

Kleinegris, D.M.M., van Es, M.A., Janssen, M., Brandenburg, W.A. & Wijffels, R.H. (2010) Carotenoid fluorescence in *Dunaliella salina*. *J. Appl. Phycol.* **22**(5), 645–649.

Kraus, G.H. & Weis, E. (1991) Chlorophyll fluorescence and photosynthesis: the basics. *Annu. Rev. Plant Physiol. Plant Mol. Biol.* **42**, 313–349.

Krishnamurthy, N. & Soots, V. (1971). Raman spectrum of gypsum. *Can. J Phys.* **49**, 885–896.

Kubo, Y., Ikeda, T., Yang, S.Y. & Tsuboi, M. (2000). Orientation of carotenoid molecules in the eyespot of algae: *in situ* polarized resonance Raman spectroscopy. *Appl. Spectrosc.* **54**, 1114–1119.

Langevin, Y., Poulet, F., Bibring, J-P. & Gondet, B. (2005). Sulfates in the north polar region of Mars detected by OMEGA/Mars express. *Science* **307**, 1584–1586.

Leybourne, M.I., Denison, R.E., Cousens, B.L., Bezys, R.K., Gregoire, D.C., Boyle, D.R. & Dobrzanski, E. (2007). Geochemistry, geology, and isotopic (Sr, S, and B) composition of evaporites in the Lake St. Martin impact structure: new constraints on the age of melt rock formation. *Geochem. Geophys. Geosyst.* **8**, 1–22. DOI: 10.1029/2006GC001481.

Lim, D. (2002). *Microbiology*, 3rd edn. Kendall/Hunt Publishing Company, Dubuque, Iowa.

Lopez-Reyes, G. *et al*. (2013). Analysis of the scientific capabilities of the ExoMars Raman Laser Spectrometer instrument. *Eur. J. Mineral.* **25**, 721–733.

Lutz, M. (1974). Resonance Raman spectra of chlorophyll in solution. *J. Raman Spectrosc.* **2**, 497–516.

Marshall, C.P. & Marshall, A.O. (2010). The potential of Raman spectroscopy for the analysis of diagenetically transformed carotenoids. *Philos. Trans. R. Soc. A: Math. Phys. Eng. Sci.* **368**(1922), 3137–3144.

Martinez-Frias, J., Amaral, G. & Vázquez, L. (2006). Astrobiological significance of minerals on Mars surface environment. *Rev. Environ. Sci. Biotechnol.* **5**, 219–231.

Massé, M., Bourgeois, O., Mouélic, S., Verpoorter, C., Le Deit, L. & Bibring, J.P. (2010). Martian polar and circum-polar sulfate-bearing deposits: sublimation tills derived from the north polar cap. *Icarus* **209**, 434–451.

McCabe, H.R. & Bannatyne, B.B. (1970). Lake St. Martin crypto-explosion crater and geology of surrounding area. *Geolog. Surv. Manitoba* **3**, 70–79.

McKay, C.P. (1997). The search for life on Mars. *Orig. Life Evol. Biosph.* **27** (1–3), 263–289.

Merzlyak, M.N., Gitelson, A.A., Chiykunova, O.B., Solovchenko, A.E. & Pogosyan, S.I. (2003). Application of reflectance spectroscopy for analysis of higher plant pigments. *Russ. J. Plant Physiol.* **50**(5), 704–710.

Milliken, R.E., Grotzinger, J.P. & Thomson, B.J. (2010). Paleoclimate of Mars as captured by the stratigraphic record in Gale Crater. *Geophys R. Lett.* **37**, L04201.

Morris, R.V., Lauer, H.V., Lawson, C.A., Gibson, E.K., Nace, G.A. & Stewart, C. (1985). Spectral and other physicochemical properties of sub-micron powders of hematite, maghemite, magnetite, goethite, and lepidocrocite. *J. Geo. Phys. Res.* **90**(B4), 3126–3144.

Murchie, S.L. *et al*. (2009). A synthesis of Martian aqueous mineralogy after 1 Mars year of observations from the Mars reconnaissance orbiter. *J. Geo. Phys. Res.* **114**, E00D06.

Panieri, G., Lugli, S., Manzi, V., Palinska, K.A. & Roveri, M. (2008). Microbial communities in Messinian evaporite deposits of the Vena del Gesso (northern Apennines, Italy). *Stratigraphy* **5**, 343–352.

Panieri, G., Lugli, S., Manzi, V., Schreiber, B.C., Palinska, K.A. & Roveri, M. (2010). Ribosomal RNA gene fragments from fossilized cyanobacteria identified in primary gypsum from the late Miocene, Italy. *Geobiology* **8**, 101–111.

Preston, L.J. & Dartnell, L.R. (2014). Planetary habitability: lessons learned from terrestrial analogues. *Int. J. Astrobiol.* **13**(01), 81–98.

Poch, O., Noblet, A., Stalport, F., Correia, Grand, N., Szopa, C. & Coll, P. (2013). Chemical evolution of organic molecules under Mars-like UV radiation conditions simulated in the laboratory with the MOMIE setup. *Planet. Space Sci.* **85**, 188–197.

Quesada, A., Vincent, W.F. & Lean, D.R.S. (1999). Community and pigment structure of Arctic cyanobacterial assemblages: the occurrence and distribution of UV-absorbing compounds. *FEMS Microb. Ecol.* **28**, 315–323.

Raulin, F. & McKay, C.P. (2002). The search for extraterrestrial life and prebiotic chemistry. *Planet. Space Sci.* **50**, 655–655.

Richardson, L.L. (1995). Remote sensing of algal bloom dynamics. *BioScience* **46**(7), 492–501.

Robert, B., Frank, H.A., Young, A.J., Britton, G. & Cogdell, R.J. (1999). *The Photochemistry of Carotenoids*, pp. 189. Kluwer Academic Publishers, Dordrecht, The Netherlands.

Schloss, P.D., Westcott, S.L., Ryabin, T., Hall, J.R., Hartmann, M., Hollister, E.B., Lesniewski, R.A., Oakley, B.B., Parks, D.H., Robinson, C.J. *et al*. (2009). Introducing mothur: open-source, platform-independent, community-supported software for describing and comparing microbial communities. *Appl. Environ. Microbiol.* **75**(23), 7537–7541.

Schloss, P.D., Gevers, D. & Westcott, S.L. (2011). Reducing the effects of PCR amplification and sequencing artifacts on 16S rRNA-based studies. *PLoS ONE* **6**(12), e27310–e27310.

Schmieder, M., Jourdan, F., Tohver, E., Mayers, C., Frew, A. & Cloutis, E. (2013). The age of the lake Saint Martin impact structure (Manitoba, Canada). *44th Lunar and Planetary Science Conference (abstract)*.

Schopf, J.W., Farmer, J.D., Foster, I.S., Kudryavtsev, A.B., Gallardo, V.A. & Espinoza, C. (2012). Gypsum-permineralized microfossils and their relevence to the search for life on Mars. *Astrobiology* **12**(7), 619–633.

Seager, S., Turner, E.L., Schafer, J. & Ford, E.B. (2005). Vegetation's Red Edge: a possible spectroscopic biosignature for extraterrestrial life. *Astrobiology* **5**(3), 372–389.

Seckback, J. (Ed). (1999). *Enigmatic Microorganisms and Life in Extreme Environments*. Kluwer Academic Publishers, Dordrecht, The Netherlands.

Sefton-Nash, E., Catling, D.C., Wood, S.E., Grindrod, P.M. & Teanby, N.A. (2012). Topographic, spectral, and thermal inertia analysis of interior layered deposits in Iani Chaos, Mars. *Icarus* **221**, 20–42.

Sherman, D.M. & Waite, T.D. (1985). Electronic spectra of Fe^{3+} oxides and oxide hydroxides in the near IR to UV. *Am. Mineral.* **70**, 1262–1269.

Shibata, Y., Saga, Y., Tamiaki, H. & Itoh, S. (2007). Polarized fluorescence of aggregated bacteriochlorophyll *c* and baseplate bacteriochlorophyll *a* in single chlorosomes isolated from *Chloroflexus aurantiacus*. *Am. Chem. Soc.* **46**, 7062–7068.

Sigler, W.V., Bachofen, R. & Zeyer, J. (2003). Molecular characterization of endolithic cyanobacteria inhabiting exposed dolomite in central Switzerland. *Environ. Microbiol.* **5**(7), 618–627.

Simoneit, B.R.T. (2004). Prebiotic organic synthesis under hydrothermal conditions: an overview. *Adv. Space Res.* **33**, 88–94.

Squier, A.H., Hodgson, D.A. & Keely, B.J. (2004). A critical assessment of the analysis and distributions of scytonemin and related UV screening pigments in sediments. *Org. Geochem.* **35**, 1221–1228.

Squyres, S.W. *et al*. (2012). Ancient impact and aqueous processes at Endeavour Crater, Mars. *Science* **336**, 570–576.

Stivaletta, N., López-García, P., Boihem, L. & Barbieri, R. (2010). Biomarkers of endolithic communities within gypsum crusts (Southern Tunisia). *Geomicrobiol. J.* **27**, 101–110.

Stoker, C.R. & Bullock, M.A. (1997). Organic degradation under simulated Martian conditions. *J. Geo. Phys. Res.* **102**(E5), 10881–10888.

Stromberg, J.M., Applin, D.M., Cloutis, E.A., Rice, M., Berard, G. & Mann, P. (2014). The persistence of a chlorophyll spectral bio signature from Martian evaporite and spring analogues under Mars-like conditions. *Int. J. Astrobiol.* **13**(3), 203–223.

Strommen, D.P. & Nakamoto, K. (1977). Resonance Raman spectroscopy. *J. Chem. Educ.* **54**, 474.

Summons, R.E., Amend, J.P., Bish, D., Buick, R., Cody, G.D., Des Marais, D.J., Dromart, G., Eigenbrode, J.L., Knoll, A.H. & Sumner, D.Y. (2011). Preservation of Martian organic and environmental records: final repost of the Mars biosignature working group. *Astrobiology* **22**(2), 157–181.

Suo, Z., Avci, R., Schweitzer, M.H. & Deliorman, M. (2007). Porphyrin as an ideal biomarker in the search for extraterrestrial life. *Astrobiology* **7**(4), 605–615.

van Amerongen, H., Vasemel, H. & van Grondelle, R. (1988). Linear dichroism of chlorosomes from *Chloroflexus aurantiacus* in compressed gels and electric fields. *Biophys. J.* **54**, 65–76.

van Amerongen, H., van Haeringen, B., van Gurp, M. & van Grondelle, R. (1991). Polarized fluorescence measurements on ordered photosynthetic antenna complexes. *Biophys. J.* **59**, 992–1001.

Vasmel, H., van Dorssen, R.J., Vasmel, H. & Amesz, J. (1986) Pigment organization and energy transfer in the green photosynthetic bacterium *Chloroflexus aurantiacus*. *Photosynth. Res.* **9**, 33–45.

Villar, S.E., Edwards, H.G.M. & Benning, L.G. (2006). Raman spectroscopic and scanning electron microscopic analysis of a novel biological colonization of volcanic rocks. *Icarus* **184**, 158–169.

Wardlaw, N.C., Stauffer, M.R. & Hoque, M. (1969). Striations, giants grooves, and superposed drag folds, Interlake area, Manitoba. *Can. J. Earth Sci.* **6**(4), 577–593.

Wierzchos, J., Ascaso, C. & McKay, C.P. (2006). Endolithic cyanobacteria in halite rocks from the hyper arid core of the Atacama Desert. *Astrobiology* **6** (3), 415–422.

Wierzchos, J., Mara, B.C.A., De Los Rios, A., Davila, A.F., Sanchez-Almazo, I.M., Artieda, O., Wierzchos, K., Gomez-Silva, B., McKay, C.P. & Ascaso, C. (2011). Microbial colonization of Ca-sulfate crusts in the hyper arid core of the Atacama Desert: implications for the search for life on Mars. *Geobiology* **9**, 44–60.

Wray, J.J. *et al*. (2010). Identification of the Ca-sulfate bassanite in Mawrth Vallis, Mars. *Icarus* **209**, 416–421.

Wray, J.J. *et al*. (2011). Columbus crater and other possible groundwater-fed paleolakes of Terra Sirenum, Mars. *J. Geophys. Res.* **116**, E01001.

Wynn-Williams, D.D., Edwards, H.G.M. & Garcia-Pichel, F. (1999). Functional biomolecules of Antarctic stromatolitic and endolithic cyanobacterial communities. *Eur. J. Phycol.* **34**(4), 381–391.

Yamada, T., Sekiguchi, Y., Hanada, S., Imachi, H., Ohashi, A., Harada, H. & Kamagata, Y. (2006). *Anaerolinea thermolimosa* sp. nov., *Levilinea saccharolytica* gen. nov., sp. nov. and *Leptolinea tardivitalis* gen. nov., sp. nov., novel filamentous anaerobes, and description of the new classes *Anaerolineae* classis nov. and *Caldilineae* classis nov. in the bacterial phylum *Chloroflexi*. *Int. J. Syst. Evol. Microbiol.* **56**(6), 1331–1340.

Ziolkowski, L.A., Mykytczuk, N.C.S., Omelon, C.R., Johnson, H., Whyte, L.G. & Slater, G.F. (2013). Arctic gypsum endoliths: a biogeochemical characterization of a viable and active microbial community. *Biogeosciences* **10**(11), 7661–7675.